

Crystal Structure and Magnetic Properties of a New Form of $\text{NH}_4\text{MnFeF}_6$

M. LEBLANC, G. FERREY, Y. CALAGE,* AND R. DE PAPE

Laboratoire des Fluorures et Oxyfluorures Ioniques, ERA 609, and

** Laboratoire Mössbauer, ERA 682, Faculté des Sciences, Route de Laval, 72017 Le Mans, Cedex, France*

Received August 2, 1982; and in revised form October 11, 1982

The hydrothermal synthesis at 380°C, 200 MPa of $\text{NH}_4\text{MnFeF}_6$, $\text{NH}_4\text{MnCrF}_6$, and RbMnFeF_6 leads to a new $AM^II M^III F_6$ structural type of orthorhombic symmetry with $Z = 8$. Lattice constants are found to be, respectively, $a = 7.844$ (4), $b = 12.819$ (8), $c = 10.582$ (6); $a = 7.808$ (5), $b = 12.755$ (9), $c = 10.501$ (7); and $a = 7.913$ (5), $b = 12.858$ (9), $c = 10.619$ (5). The structure was solved for $\text{NH}_4\text{MnFeF}_6$ from 755 X-Ray reflections and refined to $R_w = 0.029$ in the space group $Pb2n-C_{2v}^6$. The network is built from edge-sharing MnFeF_{10} bioctahedra connected to each other by their vertices. RbMnFeF_6 upon heating transforms irreversibly to the modified pyrochlore structure at 881 K. From magnetic and Mössbauer experiments, $\text{NH}_4\text{MnFeF}_6$ and $\text{NH}_4\text{MnCrF}_6$ are established to be antiferromagnetic with $T_N = 117.7 \pm 0.5$ K and < 6 K, respectively.

Introduction

Transition metal fluorides $AM^II M^III F_6$ crystallize in various structural forms: trirutile, modified pyrochlore, tetragonal bronze, or trigonal Na_2SiF_6 types. To obtain new structural species for this composition, hydrothermal synthesis—which frequently favors the growth of metastable or low temperature forms—was applied to the crystallization of $\text{NH}_4\text{MnFeF}_6$, $\text{NH}_4\text{MnCrF}_6$, and RbMnFeF_6 .

Experimental

Prismatic single crystals of $\text{NH}_4\text{MnFeF}_6$, $\text{NH}_4\text{MnCrF}_6$, and RbMnFeF_6 were grown by hydrothermal synthesis. The method was previously described (1): binary transition metal fluorides MnF_2 and FeF_3 or CrF_3 are mixed with 5 M RbF or NH_4F solutions

($AF/M'F_2/M''F_3 = 1/1/1$) in a platinum tube. After heating at 360°C, 200 MPa, for 3 days, and cooling of the autoclave, the crystals were isolated and characterized. Fluorine was analysed with a specific electrode, and metals by atomic absorption spectrometry (Table I).

Laue and Buerger precession photographs of the crystals show that reflections are consistent with space group $Pbcn-D_{2h}^{14}$. Refined lattice parameters (Å) are given in Table II, powder diffraction data for $\text{NH}_4\text{MnCrF}_6$ are presented in Table III.

$\text{NH}_4\text{MnFeF}_6$ was used for the X-ray structure determination. Intensity data were collected on a CAD 4 Nonius diffractometer¹ with $\text{MoK}\alpha$ radiation in the range

¹ Laboratoire de Cristalochimie Minérale (Professeur HARDY), Faculté des Sciences, Université de Poitiers (France).

TABLE I
CHEMICAL ANALYSIS AND SPECIFIC
GRAVITY OF $\text{NH}_4\text{MnFeF}_6$

	Exp.	Calc.
Mn	20.9(1.7) ^a	22.6
Fe	23.9(1.9)	23.0
F	47.9(2.4)	47.0
ρ	3.04(5)	3.03

^a Chemical analysis in wt% (specific gravity in g/cm^3).

$-9 \leq h \leq +9$, $-15 \leq k \leq +15$, $0 \leq l \leq 12$ with no restrictive conditions. Operating features were graphite monochromator, $3^\circ \leq \theta \leq 25^\circ$; scan mode, $\omega-2\theta$; scan range, $s = (1.80 + 0.45 \tan 2\theta)^\circ$; scintillation counter aperture, 3.00 mm; scanning speed, $v = (20.1166/NV)^\circ \text{min}^{-1}$ with NV integers.

Intensities treatment and structure determination were carried out with SHELX program (2). A total of 2807 reflections were corrected for absorption, using the numerical Gauss method; the transmission factor varied from 0.594 to 0.432. Averaging, in the Laue group mmm , leads to 755 independent reflections with $|F|/\sigma(|F|) \geq 6$. The atomic scattering factors were taken from "International Tables for X-ray Crystallography" (1968) for N° , F^- , Fe^{3+} , Mn^{2+} (3).

Structure Determination

Direct methods, using triple phase relations between F_{hkl} , were tested in the centrosymmetric $Pbcn$ space-group. After F_{hkl} ($l = 2n + 1$) renormalisation they yielded a

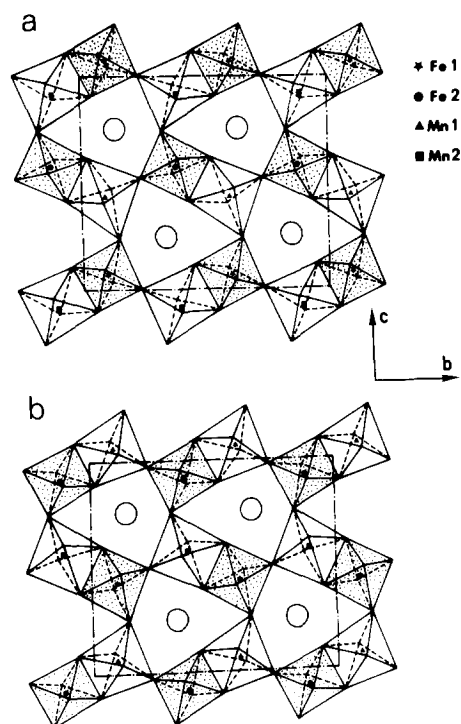


FIG. 1. Projections of $\text{NH}_4\text{MnFeF}_6$ along $[100]$ at $x = \frac{1}{4}$ (a) and $x = \frac{3}{4}$ (b); MnF_6 octahedra are dotted.

solution with a good figure of merit. Metallic atoms were located from the corresponding E map. The Fourier map, built from the set of refined metallic coordinates ($R = 0.315$) provided information on the location of fluorine and nitrogen atoms. Refinement of positional and isotropic thermal parameters for all nonhydrogen atoms, of secondary extinction and weighting, did not yield a satisfactory R value ($R = 0.210$). This fact, in spite of the lack of a piezoelectric signal, lead us to consider the noncentric space groups derived from $Pbcn$: non-

TABLE II

		a	b	c
Symmetry: orthorhombic	$\text{NH}_4\text{MnFeF}_6$	7.844(4)	12.819(8)	10.582(6)
Space group: $Pb2n - C_{2v}^6$ ($n^\circ 30$)	$\text{NH}_4\text{MnCrF}_6$	7.808(5)	12.755(9)	10.501(7)
$Z = 8$	RbMnFeF_6	7.913(5)	12.858(9)	10.619(5)

TABLE III
LATTICE SPACINGS AND OBSERVED X-RAY
INTENSITIES FOR $\text{NH}_4\text{MnCrF}_6$

hkl	I_{obs}	d_{obs}	d_{calc}
0 2 0	15	6.382	6.378
0 2 1	60	5.446	5.451
0 0 2	65	5.246	5.250
1 2 1	4	4.461	4.470
1 0 2	4	4.342	4.357
0 2 2	6	4.049	4.054
2 0 0	100	3.894	3.904
2 2 0	10	3.325	3.330
0 4 0	95	3.188	3.189
2 2 1	5	3.171	3.174
2 0 2	35	3.130	3.133
0 2 3	90	3.068	3.069
0 4 2	10	2.725	2.726
0 0 4	4	2.627	2.625
1 4 2	4	2.572	2.573
2 1 3	2	2.546	2.553
3 1 1	15	2.470	2.478
2 4 0			2.470
1 1 4	5	2.441	2.442
0 2 4	25	2.428	2.428
1 5 0			2.425
2 4 1	8	2.403	2.404
1 5 1	5	2.359	2.363
0 4 3			2.357
3 1 2	10	2.291	2.294
2 0 4	5	2.178	2.178
1 3 4	5	2.148	2.148
2 1 4			2.147
0 6 0	8	2.126	2.126
0 6 1	15	2.084	2.084
2 2 4	10	2.061	2.062
3 1 3			2.061
2 4 3	4	2.017	2.018
0 2 5	20	1.995	1.995
1 5 3			1.993
0 6 2	15	1.970	1.971
4 0 0	40	1.950	1.952
1 6 2	4	1.911	1.911

standard $P2_1cn-C_{2v}^9$, $Pb2n-C_{2v}^6$, $Pbc2_1-C_{2v}^5$. Refinement of the structure with anisotropic thermal parameters for metallic atoms permitted selection of the $Pb2n$ space group. Refinement in the two other space groups lead to nondefinite thermal vibration ellipsoids. Manganese and iron atom loca-

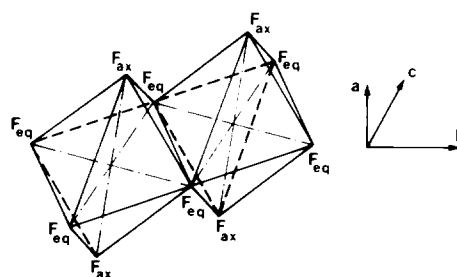


FIG. 2. MnFeF_{10} unit in $\text{NH}_4\text{MnFeF}_6$

tions were deduced from metal-fluorine distances; this technique was used recently by Banks *et al.* (4) in the crystal structure determination of the tetragonal bronze-like phase KMnFeF_6 . The residual fell to $R = 0.021$ ($R_w = 0.029$) with refinement of anisotropic thermal parameters for all non-hydrogen atoms.² Attempts to solve the true structure were unsuccessful.

Table IV presents the final results for the 20 independent positions. Characteristic interatomic distances are given in Table V.

Discussion of the Structure

Figure 1 presents the (100) projection of the structure at $x = \frac{1}{4}$ and $x = \frac{3}{4}$. The three-dimensional network may be described in terms of binuclear MnFeF_{10} groups formed by edge-sharing iron and manganese octahedra. Figure 2 shows this unit, its location with respect to the axes, and the so-called equatorial and axial fluorine atoms. These

² See NAPS document No. 04026 for 5 pages of supplementary material. Order from ASIS/NAPS. Microfiche Publications, P.O. Box 3513, Grand Central Station, New York, NY 10163. Remit in advance \$4.00 for microfiche copy or for photocopy, \$7.75 up to 20 pages plus \$30 for each additional page. All orders must be prepaid. Institutions and Organizations may order by purchase order. However, there is a billing and handling charge for this service of \$15. Foreign orders add \$4.50 for postage and handling, for the first 20 pages, and \$1.00 for additional 10 pages of material. \$1.50 for postage of any microfiche orders.

TABLE IV
FINAL ATOMIC COORDINATES AND EQUIVALENT
TEMPERATURE FACTORS IN $\text{NH}_4\text{MnFeF}_6^{a,b}$

Atom	Site	x	y	z	Beq. (\AA^2)
Fe1	4c	0.2489(1)	0.1	0.0737(1)	0.71(9)
Fe2	4c	0.2502(1)	0.3775(1)	0.5745(1)	0.50(8)
Mn1	4c	0.7509(1)	0.0956(2)	0.0719(1)	0.79(9)
Mn2	4c	0.7504(1)	0.3817(2)	0.5718(1)	0.59(8)
F1	4c	0.2069(4)	0.1492(4)	0.2439(4)	1.43(15)
F2	4c	0.2781(3)	0.4533(2)	0.1131(2)	1.04(13)
F3	4c	0.2219(4)	0.5247(4)	0.6162(4)	1.33(15)
F4	4c	0.2894(5)	0.2397(3)	0.5188(3)	1.52(15)
F5	4c	0.0121(5)	0.1156(4)	0.0360(5)	1.95(15)
F6	4c	0.0103(4)	0.3634(4)	0.5397(4)	1.20(13)
F7	4c	0.2223(4)	0.3249(3)	0.7432(4)	1.00(14)
F8	4c	0.7178(4)	0.4317(3)	0.0982(4)	1.12(15)
F9	4c	0.7739(4)	0.5478(3)	0.6000(4)	1.03(14)
F10	4c	0.7063(4)	0.2393(2)	0.4897(2)	1.74(14)
F11	4c	0.4900(4)	0.0837(3)	0.1049(5)	1.52(16)
F12	4c	0.4877(4)	0.3887(3)	0.6091(4)	1.48(15)
AM1	2a	0	0.3423(5)	$\frac{1}{4}$	1.23(12)
AM2	2a	0	-0.1838(5)	$\frac{1}{4}$	0.87(20)
AM3	2b	0	0.1201(6)	$\frac{3}{4}$	1.98(12)
AM4	2b	0	-0.3288(6)	$\frac{3}{4}$	1.95(23)

^a Estimated standard deviations are given in parenthesis.

^b Wyckoff notation, symmetry, and coordinates of general and special equivalent positions for $Pb2n$ space group

4c	1	x y z	$\frac{1}{2} - x \frac{1}{2} + y z$
		$\bar{x} y \frac{1}{2} - z$	$\frac{1}{2} + x \frac{1}{2} + y \frac{1}{2} - z$
2b	2	0 y $\frac{3}{4}$	$\frac{1}{2} \frac{1}{2} + y \frac{3}{4}$
2a	2	0 y $\frac{1}{4}$	$\frac{1}{2} \frac{1}{2} + y \frac{1}{4}$

bioctahedra, slightly tilted from the a axis (approximately 13°), are linked to six similar groups by opposite equatorial vertices along b and c , and by axial vertices along a . At $x = \frac{1}{4}$ and $x = \frac{3}{4}$, they build infinite layers

TABLE V
CHARACTERISTIC INTERATOMIC DISTANCES (\AA) IN
 $\text{NH}_4\text{MnFeF}_6$

Octahedron of Fe(1)		Octahedron of Fe(2)	
Fe1-F1	1.936(4)	Fe2-F3	1.949(4)
Fe1-F2	1.939(3)	Fe2-F4	1.891(4)
Fe1-F5	1.916(4)	Fe2-F6	1.919(3)
Fe1-F9	1.962(4)	Fe2-F7	1.922(3)
Fe1-F10	1.937(4)	Fe2-F8	1.978(3)
Fe1-F11	1.927(3)	Fe2-F12	1.909(3)
$\bar{d}_{\text{Fe1-F}}$	= 1.936	$\bar{d}_{\text{Fe2-F}}$	= 1.928
$d_{\text{F2-F9}}$	= 2.568(6)	$d_{\text{F3-F8}}$	= 2.629(6)
$\bar{d}_{\text{F-F}}$	= 2.734	$\bar{d}_{\text{F-F}}$	= 2.726
Octahedron of Mn(1)		Octahedron of Mn(2)	
Mn1-F1	2.096(4)	Mn2-F2	2.175(3)
Mn1-F3	2.199(4)	Mn2-F6	2.084(3)
Mn1-F4	2.099(4)	Mn2-F7	2.095(3)
Mn1-F5	2.095(4)	Mn2-F9	2.125(4)
Mn1-F8	2.157(3)	Mn2-F10	2.059(4)
Mn1-F11	2.083(3)	Mn2-F12	2.094(3)
$\bar{d}_{\text{Mn1-F}}$	= 2.121	$\bar{d}_{\text{Mn2-F}}$	= 2.105
$\bar{d}_{\text{F-F}}$	= 2.996	$\bar{d}_{\text{F-F}}$	= 2.974

connected by axial F_{ax} , with alternating tiltings along three axes and alternating (Mn, Fe) disposition along a and c . Thus, each metallic octahedron is surrounded by five octahedra of the other metallic species. Ammonium ions adopt 12 coordination, existing in hexagonal close packing.

The large difference between ionic radii

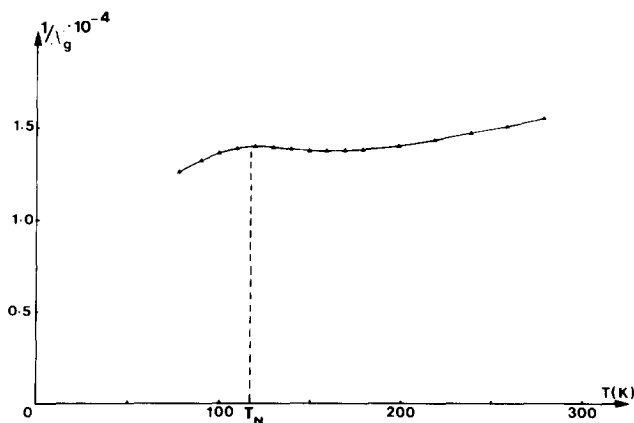


Fig. 3. Thermal variation of the inverse magnetic susceptibility ($1/\chi g^{-1}$) of $\text{NH}_4\text{MnFeF}_6$.

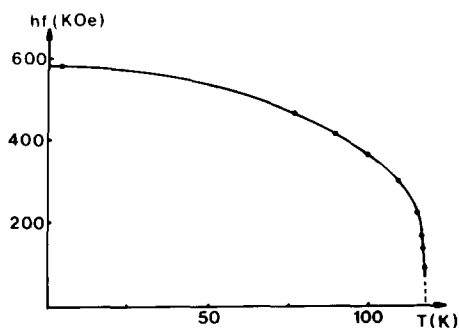


FIG. 4. Thermal variation of the magnetic hyperfine field for $\text{NH}_4\text{MnFeF}_6$.

of Mn^{2+} (0.83 Å) and Fe^{3+} (0.64 Å) (5) implies a strong distortion of both metallic octahedra (Table V).

Further distance considerations show that the fluorine atoms which form the edge between manganese and iron octahedra present the shortest fluorine-fluorine distances, but correspond to the longest metal-fluorine distances (Table V).

Very few fluorides with $M_2\text{F}_{10}$ units are known. In $\text{Ba}_2\text{Ni}_3\text{F}_{10}$ (6) these groups connect planes containing rutile chains. In BaMnFeF_7 (7), FeF_6 octahedra ensure bridging between Mn_2F_{10} entities. By contrast, numerous oxides, particularly niobates or tantalates, adopt a wide range of structures containing $M_2\text{O}_{10}$ units. These groups, tied together by vertices or edges, build up *cis* or *trans* infinite files, or rings. Orthorhombic CaTa_2O_6 (8), and the high

temperature form (HT) of BaNb_2O_6 (9) furnish, respectively, examples of *cis* and *trans* files connected by vertices. Double *trans* files connected by edges are encountered in BaTi_4O_9 and in related compounds (10–13). Three membered rings form parts of the hexagonal BaTa_2O_6 structure (14).

Therefore, $\text{NH}_4\text{MnFeF}_6$ appears to be the first fluoride with *trans* chains of $M_2\text{F}_{10}$ units. Its structure is closely related to that of HT- BaNb_2O_6 , as roughly determined from X-ray powder diffraction. The structural difference relative to HT- BaNb_2O_6 derives from the cationic order between Mn^{2+} and Fe^{3+} .

Structural Transformation

At 881 K, DTA experiments on RbMnFeF_6 show an irreversible endothermic phase transition from niobate to a modified pyrochlore type structure. When a solid state reaction is carried out between 823 and 1023 K and is followed by slow cooling, the distorted modified pyrochlore RbMnFeF_6 ($a = 7.153(7)$ Å, $b = 7.434(5)$ Å, $c = 12.34(1)$ Å, $\beta = 125^\circ 64(2)$) is the only form obtained (15); by contrast, hydrothermal synthesis under our experimental conditions, always leads to the structure presently described.

$\text{NH}_4\text{MnFeF}_6$ and $\text{NH}_4\text{MnCrF}_6$ undergo decomposition before the structural transformation temperature is reached.

TABLE VI
MÖSSBAUER DATA OF $\text{NH}_4\text{MnFeF}_6$

T (K)	δ^a (mm sec ⁻¹)	ΔEQ (mm sec ⁻¹)	$4e^b$ (mm sec ⁻¹)	H (kOe)	Γ (mm sec ⁻¹)
295	0.460(2)	0.346(4)	—	—	0.30(1)
118	0.562(2)	0.391(4)	—	—	0.31(1)
77	0.56(1)	—	-0.42(4)	463(2)	0.32(1)
4.2	0.56(1)	—	-0.42(4)	581(2)	0.50(1)

^a δ = isomer shift relative to Fe metal ($T = 300$ K).

^b e = quadrupolar shift of the outer Zeeman lines.

Magnetic and Mössbauer Studies

A plot of inverse susceptibility χ^{-1} versus T for $\text{NH}_4\text{MnFeF}_6$ is shown in Fig. 3. It exhibits a flat minimum around 170 K and, even at 293 K, the Curie–Weiss law is not obeyed; thus, the molar Curie constant and θ_p value can not be obtained. Magnetization, measured by a vibrating sample magnetometer, indicates a superimposed parasitic ferromagnetism below T_N , with $\sigma_{4.2\text{K}} = 0.005(2) \mu_B \text{ mole}^{-1}$. RbMnFeF_6 displays an inverse susceptibility curve similar to that of $\text{NH}_4\text{MnFeF}_6$. $\text{NH}_4\text{MnCrF}_6$ is anti-ferromagnetic with $T_N < 6$ K, $\theta_p = -8$ K and $C_{\text{exp}} = 6.45 \pm 0.10$ ($C_{\text{th}} = 6.25$).

Mössbauer experiments on $\text{NH}_4\text{MnFeF}_6$ provided an accurate determination of $T_N = 117.7 \pm 0.5$ K and confirmed the three-dimensional magnetic ordering (16) with $\beta = 0.34$ and $D = 1.33$. As deduced from bond lengths and the consideration of angles the two types of iron III sites are very similar. They cannot be distinguished by Mössbauer spectroscopy, due to the relative insensitiveness of iron III spectrum towards the surrounding (17). The thermal variation of their common hyperfine magnetic field is shown in Fig. 4; characteristic Mössbauer data are provided in Table VI. From the ϵ values, the angle between the magnetic hyperfine field direction and the main electric field gradient axis is probably 90° .

Conclusion

In this structure, magnetic interactions proceed from superexchange coupling. Fe–

Mn angles are close to 157 , 136 and 102° . So, $\sim 180^\circ$, $\sim 90^\circ$, and intermediate couplings exist. The magnetic structure determination, scheduled at the ILL Grenoble, should specify the spin directions, particularly inside the bioctahedron, and correlate the Mössbauer resonance and magnetization results.

References

1. G. FERREY, M. LEBLANC, R. DE PAPE, M. PASARET, AND M. BOTHEREL-RAZAZI, *J. Cryst. Growth* **29**, 209 (1975).
2. G. M. SHELDRIK, SHELX, Program for crystal structure determination 1976, Univ. of Cambridge, England.
3. "International Tables for X-ray Crystallography," Vol. IV, Kynoch Press, Birmingham (1968).
4. E. BANKS, S. NAKAJIMA, AND G. J. B. WILLIAMS, *Acta Crystallogr. Sect. B* **35**, 46 (1979).
5. R. D. SHANNON, *Acta Crystallogr. Sect. A* **32**, 751 (1976).
6. M. LEBLANC, G. FERREY, AND R. DE PAPE, *J. Solid State Chem.* **33**, 317 (1980).
7. H. HOLLER, D. BABEL, M. SAMOUEL, AND A. DE KOZAK, *J. Solid State Chem.* **39**, 345 (1981).
8. L. JAHNBERG, *Acta Chem. Scand.* **71**, 2548 (1963).
9. F. GALASSO, G. LAYDEN, AND G. GANUNG, *Mat. Res. Bull.* **3**, 397 (1968).
10. K. LUKAZEWICZ's, *Roczn. Chem.* **31**, 1111 (1957).
11. A. D. WADSLEY, *Acta Crystallogr.* **17**, 623 (1964).
12. Y. PIFFARD, Thèse, 25 Nov. 1980. Nantes (France).
13. B. M. GATEHOUSE AND M. C. NESBIT, *J. Solid State Chem.* **39**, 1 (1981).
14. G. K. LAYDEN, *Mat. Res. Bull.* **3**, 349 (1968).
15. C. JACOBONI, Thèse d'Etat, Paris VI (1976).
16. G. K. WERTHEIM, "Mössbauer Effect Methodology," Vol. IV, p. 159, Plenum, New York (1968).
17. N. N. GREENWOOD, F. MENIL, AND A. TRESSAUD, *J. Solid State Chem.* **5**, 402 (1972).